02

Electroluminescence of LEDs with quantum wells at high and low-level injection

© M.A. Mintairov, V.V. Evstropov, N.A. Kalyuzhnyy, D.A. Malevskii, S.A. Mintairov, M.Z. Shvarts

Ioffe Institute, St. Petersburg, Russia

e-mail: mamint@mail.ioffe.ru

Received May 03, 2024
Revised July 27, 2024
Accepted October 30, 2024

The luminescence intensity saturation of LEDs with quantum wells at an excessive concentration of carriers in the active region has been studied. The experimental electroluminescence spectra for a LED (area 1 mm^2) based on the $Al_{0.2}Ga_{0.8}As$ *p-i-n-* junction with six $In_{0.1}Ga_{0.9}As$ quantum wells are analysed and the experimental dependence of the main peak electroluminescence intensity on current density is obtained. At low currents, this dependence is linear (proportional) and sublinear at high currents. Approximation of the sublinear region made it possible to estimate the magnitude of the current J_{sat}, at which saturation begins. The energy diagram of the quantum well is also considered and a theoretical model is proposed that makes it possible to independently calculate the value of J_{sat}. For the sample under study, the calculation showed that $J_{sat} \sim 30\,\mathrm{A/cm^2}$. In this case, the experimental value for the LED with six quantum wells was 210 A/cm^2, which in terms of one well gives 35 A/cm^2. The close correspondence between the calculated and experimental values confirms the applicability of the proposed model. An increase in the width of all electroluminescence peaks from quantum wells with increasing current was also experimentally observed.

Keywords: LED, saturation of electroluminescence intensity.

DOI: 10.61011/EOS.2024.12.60438.6601-24

Semiconductors III–V are widely used as materials to make light diodes of various practical use [1]. Besides, to form the active area of light diodes, often quantum wells (QWs) are used, which improves their internal quantum efficiency [2]. It is known that such structures may face a problem of complete filling of the quantum well, as a result of which the dependence of luminescence intensity from current passed through the light diode aims at saturation [3–9]. In papers [3–5] the saturation area was clearly recorded, and papers [6–9] found deviation of the characteristic from the linear form and start of the trend towards saturation.

The saturation phenomenon restricts the use of light diodes where the linearity of connection is required between the intensity of electroluminescence and current through the light diode. Therefore, the determination of the saturation phenomenon patterns is of practical significance. The paper analyses the linear section (no saturation), sublinearity (trend towards saturation) and border between sections, i.e. current density J_{sat}, when saturation starts. For experimental determination J_{sat} a method is proposed, which is based on an empirical formula that describes the characteristic „intensity of luminescence — current density".

Let us consider the characteristic L–J („intensity of electroluminescence–current strength"), it contains two sections: linear and sublinear. The sections correspond to the weak and strong injection. Energy diagrams are presented in fig. 1. Current through *p-n*-transition, while there is no saturation, is caused by bimolecular recombination in QW (as, for example, shown in papers [10–12]):

$$J = q(B^{2D} + B_{nr}^{2D})n^{2D}p^{2D}, \tag{1}$$

where B^{2D} and B_{nr}^{2D} — accordingly radiative and nonradiative coefficients of bimolecular recombination, n^{2D} and p^{2D} — concentrations of 2D (2*D*) electrons and holes are expressed via Fermi quasi-levels. Intensity of bimolecular luminescence is determined by expression

$$L = B^{2D}n^{2D}p^{2D}. \tag{2}$$

From comparison of (1) and (2) it follows that the luminescence intensity (density of photon flux $\left(\frac{\text{photon}}{\text{s·cm}^2}\right)$ is proportionate to current strength, while there is no saturation (including under weak injection).

Let us consider a case of strong injection [1]. Under strong injection (contrary to the weak one) the Fermi electron quasi-level is located above the quantization level in the electron well: $F_n^{2D} > E_n$, and for the holes, on the contrary, $F_p^{2D} < E_p$ (fig. 1, *b*). In case of strong injection the concentrations of electrons and holes are expressed via Fermi quasi-levels

$$n^{2D} = N_C^{2D}\frac{F_n^{2D} - E_n}{kT}, \quad p^{2D} = N_V^{2D}\frac{E_p - F_p^{2D}}{kT},$$

where N_C^{2D}, N_V^{2D} — density of electron and hole states in the quantum well, k — Boltzmann constant, T — absolute temperature. In the limit case (the electron concentration

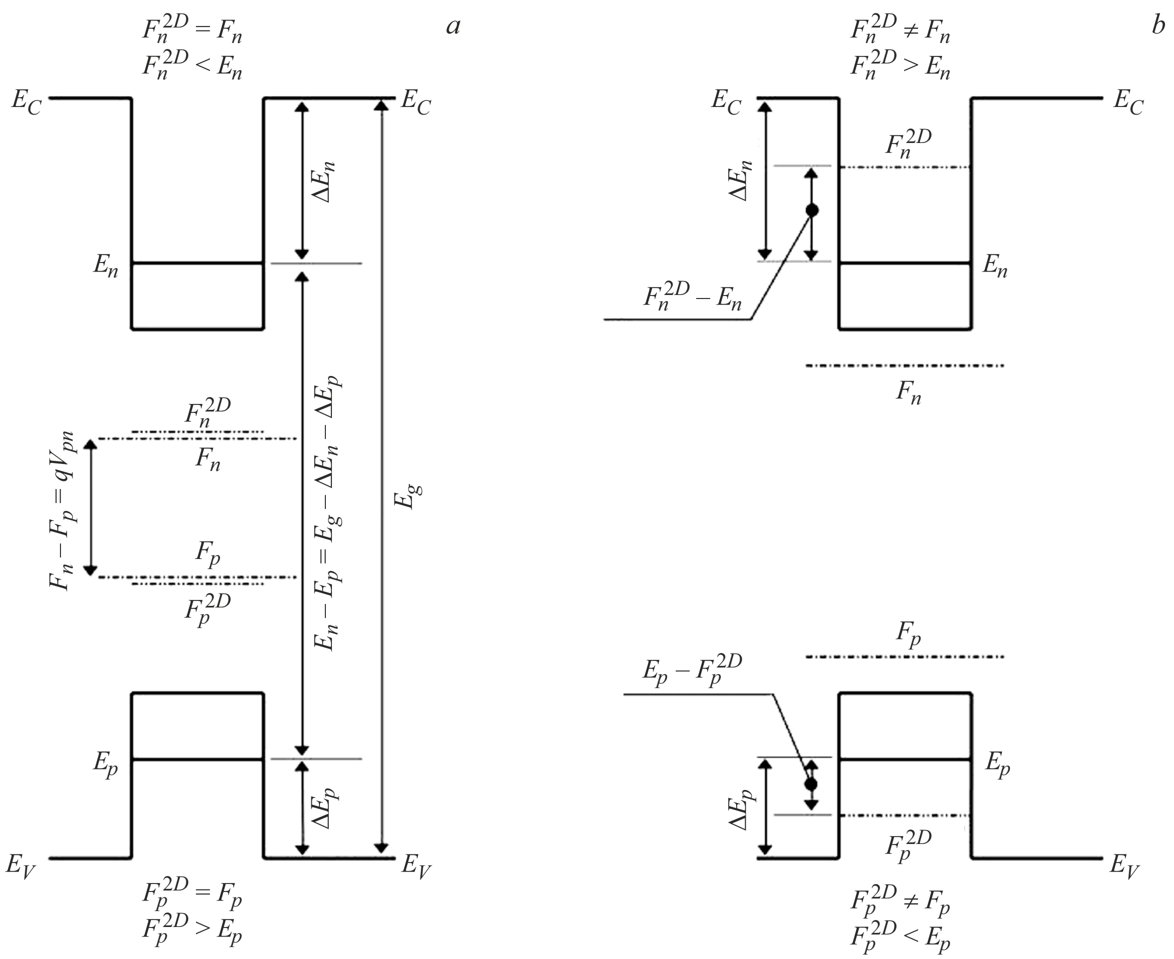

Figure 1. The general view of energy diagram of quantum well at two levels of injection: *a* — weak, *b* — strong. Note that the calculation of value J_{sat} for the studied sample used the following magnitudes of values: $E_g = 1.6734$ eV; $E_n - E_p = 1.541$ eV.

tends to density of electron states) $F_n^{2D} \to E_C$. Accordingly, $F_n^{2D} - E_n \to \Delta E_n$, $n^{2D} \to n_{sat}^{2D}$, where

$$n_{sat}^{2D} = N_C^{2D} \frac{\Delta E_n}{kT}, \tag{3a}$$

similarly

$$p_{sat}^{2D} = N_V^{2D} \frac{\Delta E_p}{kT}, \tag{3b}$$

where

$$N_C^{2D} = m_C \frac{m_0 kT}{\pi \hbar^2}, \quad N_V^{2D} = m_V \frac{m_0 kT}{\pi \hbar^2}, \tag{4}$$

where m_0 — electron mass in vacuum, $\hbar$ — Planck constant, m_C, m_V — dimensionless masses of electron and hole accordingly. In case of strong injection it is necessary to account for the neutrality condition $n^{2D} = p^{2D}$. Saturation of luminescence intensity occurs when either electron or hole well are fully filled. Then in the equation for current (1) the product of concentrations $n^{2D} p^{2D}$ is equal to the least of both values: $(n_{sat}^{2D})^2$, $(p_{sat}^{2D})^2$, where n_{sat}^{2D} and p_{sat}^{2D} — concentrations, at which the electron or hole wells are fully filled, accordingly. Current density, when the luminescence saturation occurs,

$$J_{sat} = q(B^{2D} + B_{nr}^{2D}) \times \begin{cases} (n_{sat}^{2D})^2, & \text{if } n_{sat}^{2D} < p_{sat}^{2D} \\ (p_{sat}^{2D})^2, & \text{if } n_{sat}^{2D} > p_{sat}^{2D} \end{cases} \tag{5}$$

or with account of expressions (3), (4)

$$J_{sat} = q(B^{2D} + B_{nr}^{2D}) \left(\frac{m_0}{\pi \hbar^2} \right)^2 \times \begin{cases} (m_C \Delta E_n)^2, & \text{if} \quad n_{sat}^{2D} < p_{sat}^{2D} \\ (m_V E_p)^2, & \text{if} \quad n_{sat}^{2D} > p_{sat}^{2D}. \end{cases} \tag{6}$$

Let us consider the application of the obtained expressions to the experimental structures. Light-emitting *p-i-n*-structures were created by MOVPE method (metal-organic vapor-phase epitaxy). Matrix $Al_{0.2}Ga_{0.8}As$ ($E_g = 1.6734$ eV) consists of three areas: *p*-type, electrically neutral and *n*-type. This *p-i-n*-structure is limited at both sides with wide-band barriers. In the non-doped area there are QWs $In_{0.1}Ga_{0.9}As$ with width of 3 nm. The area of the manufactured light-emitting diode based on *p-i-n*-structure was 1 mm^2.

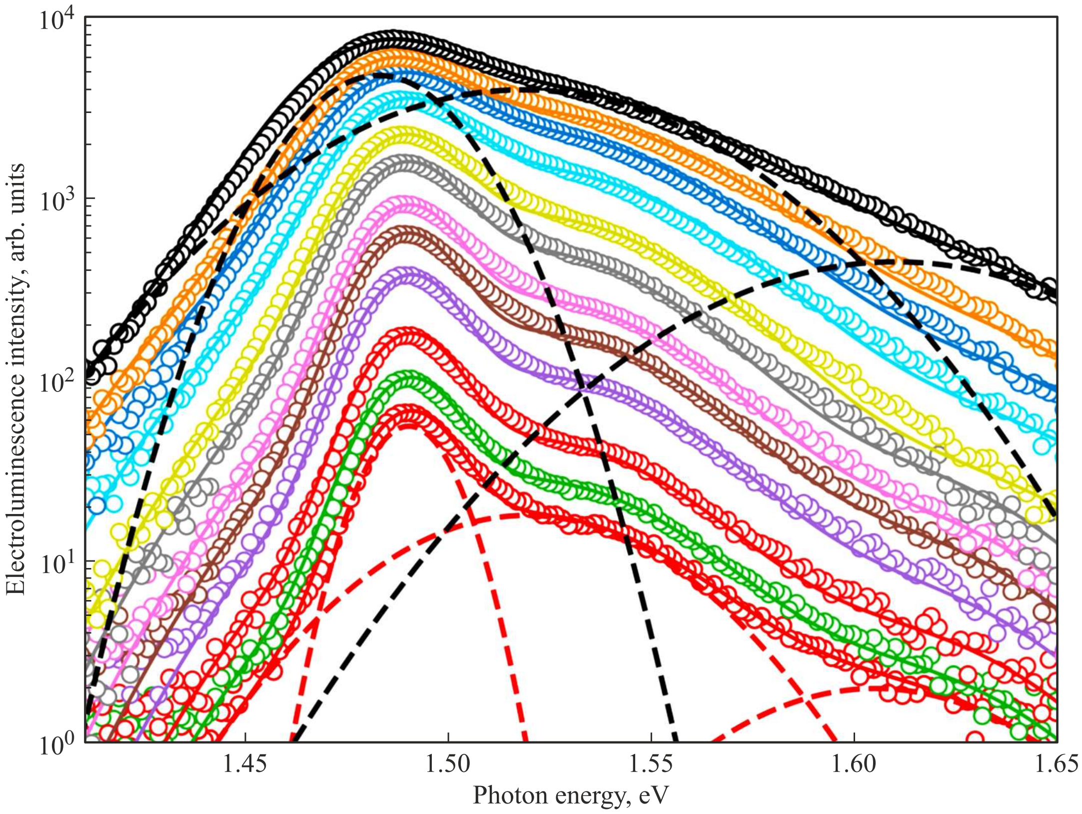

Figure 2. QW electroluminescence spectra at different currents. Circles — experimental data, solid lines of the same color — approximation using the sum of three Gaussian-shaped bands. Dashed lines show the result of spectrum decomposition into three bands: red color — at minimum measured current, black — at maximum. Current values are same as in fig. 3.

For the manufactured structure, the spectra of electroluminescence were measured in the range of the current densities from 0.2 to 500 A/cm^2. The control signal of the specified amplitude from the output of the digital-to-analog converter of the data collection system was supplied to an operational amplifier, the output of which generated a pulse of direct current and voltage applied to the tested specimen. To prevent the heating of the studied sample, a mode of a series of consequent current pulses with duration 150 μs and period 20 ms was used. To check the temperature stability within a single pulse, the constancy of the applied voltage was evaluated when the fixed current was flowing. For compliance with the dynamic range of spectrometer sensitivity, the number of pulses decreased as the current via the specimen increased, and the level of electroluminescence at the same time was reduced to single pulse.

The produced spectra of electroluminescence (fig. 2) were decomposed into Gaussian-shaped bands and included at least two bands with peaks at 1.48 and 1.54 eV. These bands correspond to radiative transitions to the levels of heavy and light holes accordingly. The main band (transition of electron−heavy hole) was studied in detail. The dependence of the integral intensity of this band on current density (fig. 3) has two areas: linear and saturated. The dependence is approximated with the empirical exponential function:

$$L = pJ_{sat}\left(1 - \exp\left(\frac{-J}{fJ_{sat}}\right)\right), \qquad (7)$$

where f — number of QWs in the non-doped area (for the studied specimen $f = 6$), p — coefficient of proportionality between the electroluminescence intensity and current density. Coefficient p was determined directly from the experimental $L{-}J$-dependence, at which the area was identified, where $L \propto J$. For the obtained experimental dependence (fig. 3) this area was located between 5 and 30 A/cm^2, and the value $p = 1.762\,\text{cm}^2/\text{A}$. Therefore, equation (7) contains one selection parameter — sought current density J_{sat}. The result of approximation by equation (7) is given in fig. 3, $J_{sat} = 35\,\text{A/cm}^2$.

Value J_{sat} was also estimated. The estimation was carried out in stages using formulae (3), (4) and the first variant of formula (5), where thermal energy $kT \sim 0.025$ eV, depth of levels were assessed using formula $\Delta E_n \sim \Delta E_p = (E_g - h\nu)/2$, where $E_g = 1.6734$ eV, $h\nu = E_n - E_p = 1.541$ eV ($h\nu$ — photon energy determined by the position of the corresponding maximum in fig. 2). Density of states was determined using formula (4), where $m_C = 0.027$, $m_V = 0.42$, $N_C^{2D} = 2.84 \cdot 10^{11}\,\text{cm}^{-2}$; $N_C^{2D} < N_V^{2D} = 4.40 \cdot 10^{12}\,\text{cm}^{-2}$.

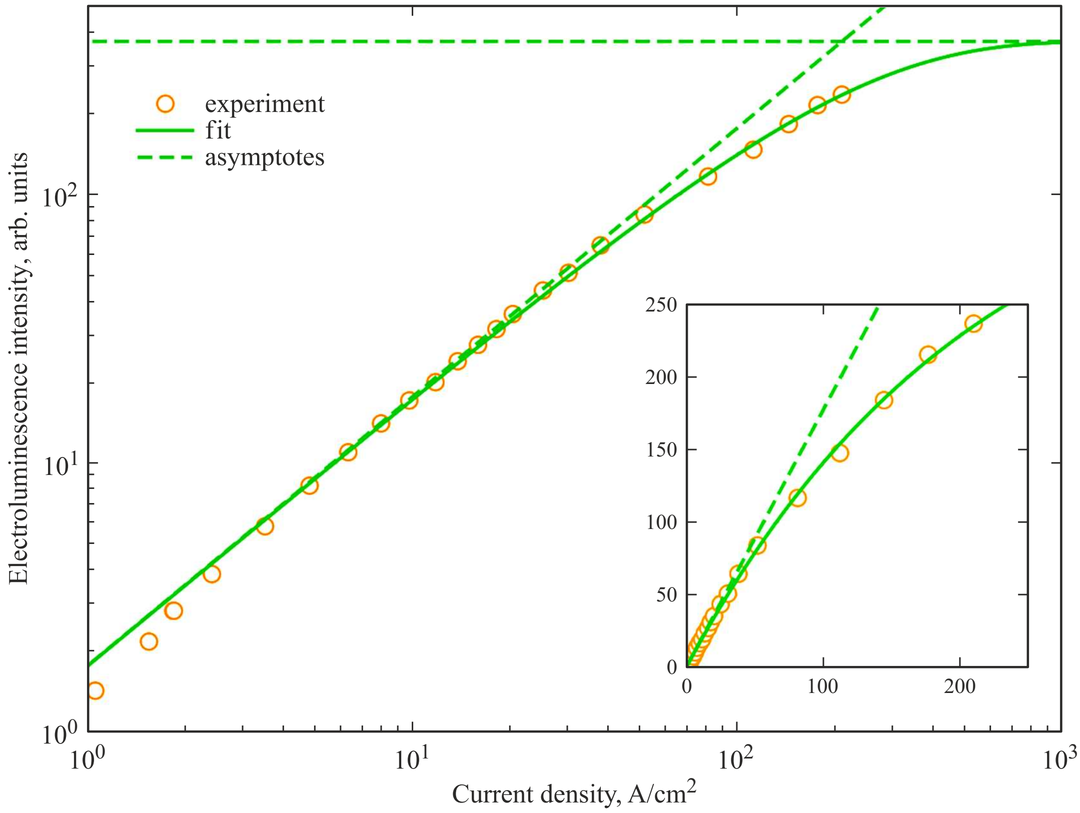

Figure 3. Dependence of integral intensity of the main band (1.48 eV) on current density: circles — experiment, solid line — result of approximation using formula (7), dashed lines — asymptotes for linear and saturated areas. Dimensions of axes on the insert are the same as in the main figure.

Electron concentration estimated by (3a) made $n^{2D}_{sat} = 7.49 \cdot 10^{11}\,\text{cm}^{-2}$. Bimolecular coefficient according to [1], $B^{2D} = B/d$, where $B = 10^{-10}\,\text{cm}^3/\text{s}$ — 3D-coefficient, $d = 3\,\text{nm}$ — width of QW, nonradiative coeffcient B^{2D}_{nr} was not taken into account. Using the above values, the estimate provides $J_{sat} \sim 30\,\text{A/cm}^2$. Note that J_{sat} is proportionate to the squared concentration of carriers, which in its turn exponentially depends on the width of the prohibited zone. Taking this into account, the experimental and estimated values are in good agreement, therefore, the empirical equation (7) is applicable. At the same time the approximation of experimental data also presumes the procedure to search for the section of proportionality in the recorded dependence $L-J$ and determination of the coefficient of proportionality p.

Therefore, the luminescence intensity saturation phenomenon was studied experimentally and by estimation at high levels of injection (at concentrations 2D-of carriers $d \sim 10^{12}\,\text{cm}^{-2}$). The method was proposed for experimental determination of current density J_{sat}, when the electroluminescence intensity saturation was observed for a single quantum well. The obtained agreement of the estimated data with the experimental data confirms the applicability of the proposed method for determination of the current density value, when electroluminescence intensity saturation starts for the light diodes with quantum wells.

Conflict of interest

The authors declare that they have no conflict of interest.

References

[1] E.F. Schubert. *Light-emitting diodes* (Cambridge University Press, 2006).
[2] A.V. Malevskaya, N.A. Kalyuzhnyy, D.A. Malevskii, S.A. Mintairov, A.M. Nadtochiy, M.V. Nakhimovich, F.Y. Soldatenkov, M.Z. Shvarts, V.M. Andreev. FTP, **55** (8), 699 (2021) (in Russian). DOI: 10.21883/{FTP}.2021.08.51143.9665
[3] M. Hirotani, T.E. Sale, J. Woodhead, J.S. Roberts, P.N. Robson, T. Saka, T. Kato. J. of Crystal Growth, **170**, 390–393 (1997). DOI: 10.1016/S0022-0248(96)00534-9
[4] N.E.J. Hunt, E.F. Schubert, D.L. Sivco, A.Y. Cho, G.J. Zydzik. Electron. Lett., **28** (23), 2169 (1992). DOI: 10.1049/el:19921392
[5] Y. Yu, X. Qin, B. Huang, J. Wei, H. Zhou, J. Pan, W. Chen, Y. Qi, X. Zhang, Z. Ren. Vacuum, **69** (4), 489–493 (2003). DOI: 10.1016/S0042-{207X}(02)00560-2

[6] H. De Neve, J. Blondelle, P. Van Daele, R. Baets, P. Demeester, G. Borghs. Electron. Lett., **30** (21),1787–1789 (1994). DOI: 10.1049/el:19941216
[7] T. Takamori, A.R. Pratt, T. Kamijoh. Appl. Phys. Lett., **74** (24), 3598–3600 (1999). DOI: 10.1063/1.123193
[8] H.-J. Lee, G.-H. Park, J.-S. So, C.-H. Lee, J.-H. Kim, L.-K. Kwac. Infrared Phys. Technol., **118**, 103879 (2021). DOI: 10.1016/j.infrared.2021.103879
[9] D.-K. Kim, H.-J. Lee. J. Nanosci. Nanotechnol., **18** (3), 2014–2017 (2018). DOI: 10.1166/jnn.2018.14952
[10] M.A. Mintairov, V.V. Evstropov, S.A. Mintairov, A.M. Nadtochiy, R.A. Saliy, M.Z. Shvarts, N.A. Kalyuzhny. Pisma v ZhTF, **46** (12), 30 (2020) (in Russian). DOI: 10.21883/{PJTF}.2020.12.49524.18284
[11] M.A. Mintairov, V.V. Evstropov, S.A. Mintairov, R.A. Salii, M. Z. Shvarts, N.A. Kalyuzhnyy. Semiconductors, **52** (10), 1244–1248 (2018). DOI: 10.1134/S1063782618100135
[12] M.A. Mintairov, V.V. Evstropov, M.Z. Shvarts, S.A. Mintairov, R.A. Salii, N.A. Kalyuzhnyy. AIP Conf. Proc., **1747**, 050003 (2016). DOI: 10.1063/1.4954366

Translated by M.Verenikina